0031-3998/90/2705-0445$02.00/0
PEDIATRIC RESEARCH

Vol. 27, No. 5, 1990
Printed in U.S.A.

Carbon Dioxide-Related Changes in Cerebral Blood Volume and Cerebral Blood Flow in Mechanically Ventilated Preterm Neonates: Comparison of Near Infrared Spectrophotometry and ^{133}Xenon Clearance

O. PRYDS, G. GREISEN, L. L. SKOV, AND B. FRIIS-HANSEN

Department of Neonatology, State University Hospital (Rigshospitalet), Copenhagen, Denmark

ABSTRACT. Carbon dioxide-induced changes in near infrared spectrophotometry recordings were compared with changes in cerebral blood flow estimated by ^{133}Xenon clearance (global cerebral blood flow (infinity)) at serial measurements in 24 mechanically ventilated preterm infants (mean gestational age 30.2 wk). In all infants, three measurements were taken at different arterial carbon dioxide tension levels (mean 4.4 kPa, range 2.1–7.8) obtained by adjustment of the ventilator settings. Mean arterial blood pressure changed spontaneously, whereas arterial oxygen tension was kept within normal range. At all wavelengths (904, 845, 805, and 775 nm), the OD increased at higher arterial carbon dioxide tension levels, indicating cerebral vasodilation. This conclusion was supported by conversion of the data to changes in oxygenated and deoxygenated Hb concentration. A parallel increase in cerebral blood volume index and global cerebral blood flow (infinity) was found ($p < 0.0001$). The oxygenation level of cytochrome aa_3 increased with increases in oxygen delivery ($p < 0.0001$). This observation, however, may have been artifactual due to cross-talk between the oxidized cytochrome aa_3 and the oxygenated Hb signals, as these signals were closely interrelated in the present experimental design. We suggest that near infrared spectrophotometry may be used for estimation of the cerebral blood volume index/cerebral blood flow-CO_2 reactivity within a wide range of arterial carbon dioxide tension. Knowledge of the light path length would put this estimation on a quantitative basis. (*Pediatr Res* 27: 445–449, 1990)

Abbreviations

CBF, cerebral blood flow
CBF_∞, global cerebral blood flow (infinity)
CBV_I, cerebral blood volume index
HbC, blood hemoglobin concentration (tetraheme molecule)
HbO_2, oxygenated hemoglobin
HbR, deoxygenated hemoglobin
HbTOT, total Hb
MABP, mean arterial blood pressure
NIRS, near infrared spectrophotometry
CI, confidence interval
$PaCO_2$, arterial carbon dioxide tension
PaO_2, arterial oxygen tension
SaO_2, arterial blood oxygen saturation

Received March 15, 1989; accepted November 28, 1989.
Correspondence: O. Pryds, Department of Neonatology, Rigshospitalet, Blegdamsvej, 2100 Copenhagen Ø, Denmark.

The method of NIRS has been proposed for noninvasive monitoring of changes in the amount of HbO_2 and HbR in the brain as well as changes in the redox level of cytochrome aa_3, the terminal member of the respiratory chain (1–3). This technique may have a particular application for the evaluation of adequate oxygen delivery to the brain of sick preterm infants, to prevent hypoxic-ischemic encephalopathy.

No prior study has tried to validate the NIRS recordings in preterm infants by cerebral physiologic variables. Therefore, we investigated how changes in CBV_I detected by NIRS were related to changes in CBF, and whether changes in saturation of brain Hb and redox level of cytochrome aa_3, respectively, were related to changes in oxygen delivery to the brain.

Carbon dioxide-induced cerebral vasodilation results in a proportional increase in CBV and CBF in experimental animals over a wide range of $PaCO_2$ (4–7). In human adults the CBV-CO_2 and CBF-CO_2 reactivities are 1:2 to 1:4 (8, 9). Therefore, our study was designed to evaluate the effect of acute changes in $PaCO_2$.

MATERIALS AND METHODS

NIRS. NIRS relies on the relative transparency of the neonate's head to near infrared light, which is attenuated by scattering and absorption in the tissues. The attenuation due to scattering may be assumed to be constant, whereas changes of absorbed light depend on changes in the chromophore concentrations (Hb and cytochrome aa_3) and the proportions of their oxygenated and deoxygenated forms. By selection of appropriate wavelengths, algorithms can be developed for the calculation of changes in HbO_2 and HbR and oxidized cytochrome aa_3, respectively (see below).

The NIRS instrument consists of four semiconductor laser diodes (class 3B) with wavelengths of 904, 845, 805, and 775 nm. The lasers are operated sequentially, and pulsed with a repetition rate of 500 Hz for 200 ns. Optical fiber bundles are used to transmit and receive the light. The energy emitted by each diode (peak power 10 W, mean power 4 mW) is several orders of magnitude below the safety limits (BS4803).

A digital computer calculates the amount of absorbed light within the head and displays the raw and converted data, respectively. The equipment was developed in Professor P. Rolfe's laboratories and made available by Radiometer (Copenhagen, Denmark).

To improve the signal to noise ratio in our study, the NIRS data were averaged over 30-s periods. From measurements on glass filters of 8 OD, a coefficient of variation of 0.01–0.04% over the 30-s period was found. System drift was less than 0.004 OD/h for all four laser diodes.

Table 1. *Relative changes (SEM) in OD* for the four wavelengths (nm) 904, 845, 805, and 775 vs changes in $PaCO_2$ and CBF_∞, respectively*†

nm	$PaCO_2$ OD change/kPa	*p*	CBF_∞ OD change/mL/100 g/min	*p*
904	0.00749 (0.00108)	< 0.0001	0.00259 (0.00042)	< 0.0001
845	0.00766 (0.00110)	< 0.0001	0.00263 (0.00044)	< 0.0001
805	0.00744 (0.00119)	< 0.0001	0.00268 (0.00045)	< 0.0001
775	0.00350 (0.0011)	0.0018	0.00166 (0.00035)	< 0.0001

* Regression coefficients.

† Results based on 72 investigations in 24 preterm neonates.

Table 2. *Mean CBF_I-CO_2 and CBF_∞-CO_2 reactivities (SEM) in 24 preterm infants**

Age	*n*	CBV_I-CO_2 (mL/100 g × cm/kPa)	*p*	CBF_∞-CO_2 (%/kPa)	*p*
D 1	13	1.46 (0.42)	0.0010	11.9 (2.3)	0.0002
D 2	11	2.06 (0.52)	0.0003	27.3 (3.9)	< 0.0001
All	24	1.70 (0.33)	< 0.0001	17.6 (2.3)	< 0.0001

* Infants were grouped according to age at investigation.

Algorithm development. The method uses the known absorption properties of Hb and the cytochrome complex. In addition, the *in vivo* extinction coefficients of the three chromophores at each of the wavelengths must be known. A minimum of three wavelengths is necessary to solve an equation with three variables; we used 775, 805, and 904 nm for the conversion to concentrations.

At each of the wavelengths, the absorbance (A) is proportional to the product of the extinction coefficient of the chromophore (e), the concentration of the chromophore (c), and the path length of the light (l). The total absorbance (A_n) at one wavelength (n) is the sum of the absorbances of the different absorbing components:

$$A_n = e_{HbRn} \times l \times c_{HbR} + e_{HbO_2n} \times l \times c_{HbO_2} + e_{Cytn} \times l \times C_{Cyt}$$

From the extinction coefficients provided by Wray *et al.* (10), the following multiplication factors were obtained by means of linear interpolation and matrix inversion:

	775 nm	805 nm	904 nm
HbO_2	−0.944	−0.126	1.441
HbR	1.554	−0.739	−0.382
cytochrome aa_3	−0.095	0.378	−0.213

Changes in concentrations of HbO_2, HbR, and cytochrome aa_3 are calculated by summation of the absorption changes from the start of monitoring (measured as OD) multiplied by the above coefficients at each of the wavelengths. Changes in HbTOT are the sum of HbO_2 and HbR. Inasmuch as at present the path length is unknown, the results are relative and expressed with the unit mM × path length in cm.

CBF. CBF was determined by the i.v. ^{133}Xe technique, validated in preterm infants with respiratory distress (11). In short, 0.5–1.0 mCi/kg ^{133}Xe was injected into a peripheral vein and the clearance recorded by scintillators placed over one frontoparietal region and the thorax, respectively. Fifteen min of recording time was used to improve the accuracy at low CBF levels (12). CBF was calculated from the time the activity in the lung had decreased to 15% of its peak activity, using the Obrist 2-compartment analysis modified to adjust for increased recirculation of tracer (12). CBF_∞ is the weighted mean of gray and white matter flow (12). The blood-brain partition coefficient was set to 0.8 mL/g as previously calculated and adjusted for blood Hb (13). Inasmuch as the neonate's head is small and the scintillation geometry allows counting from a volume of 100–200 mL, CBF_∞ is considered to represent global CBF and is expressed as mL/100 g/min. Before each of the CBF measurements, the background activity was measured (0.5 or 5 min) and taken into account in the subsequent CBF_∞ calculation.

Patients. Twenty-four preterm infants with a mean gestational age of 30.2 wk (SD 2.8) and a mean birth wt of 1380 g (SD 504) were studied. Mean Apgar score at 5 min was 8.3 (SD 1.8) and mean umbilical cord pH was 7.27 (SD 0.16). None of the infants were hypoglycemic (blood glucose <1.7 mM) at the time of the study. HbC was stable as no infant was transfused (mean tetraheme concentration 2.7 mM, SD 0.35).

Each study included three serial measurements within about 2 h. Thirteen infants were investigated during the first day of life and another 11 infants during the second day. All infants were mechanically ventilated for respiratory distress and therefore routinely sedated with phenobarbital (loading dose 15 mg/kg;

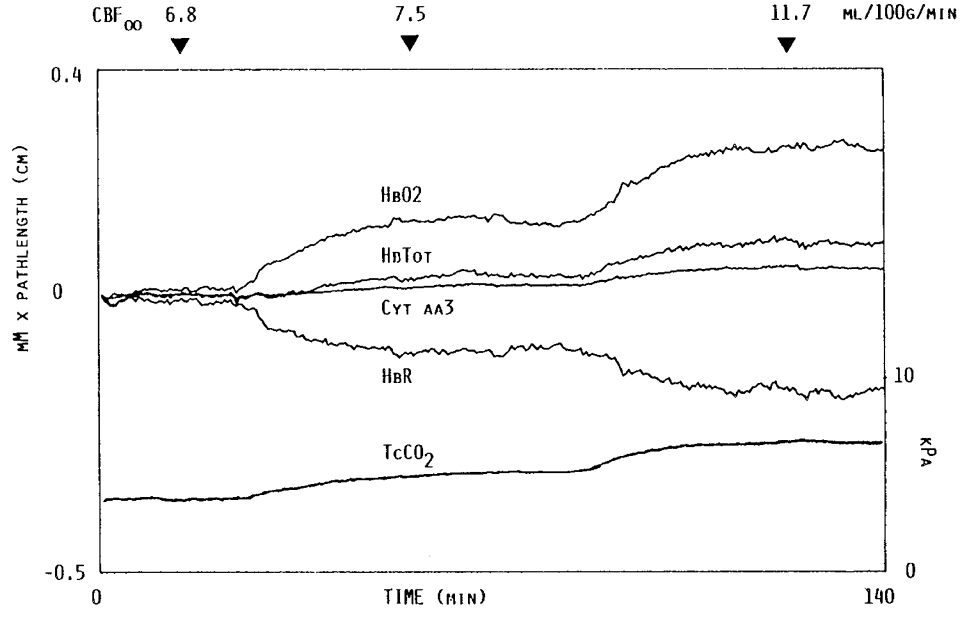

Fig. 1. Changes in relative concentrations (mM × path length) of HbTOT, HbO_2, HbR, and oxidized cytochrome aa_3 (*Cyt aa3*) *vs* changes in transcutaneous CO_2 tension ($TcCO_2$) in a representative newborn infant. CBF_∞ was measured three times during the 140-min period.

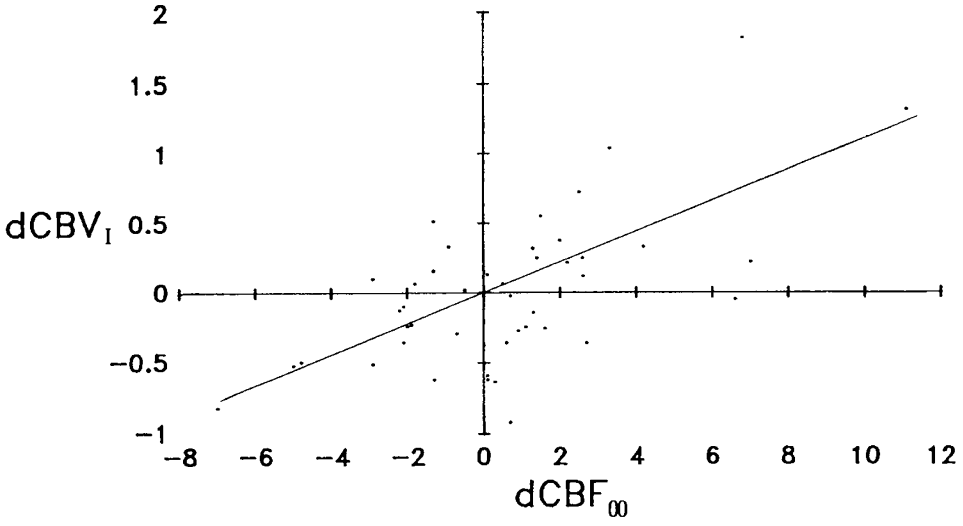

Fig. 2. Changes in CBV_I ($dCBV_I$ mL/100 g × cm) *vs* changes in CBF ($dCBF_\infty$ mL/100 g/min) in 24 preterm infants. In each infant, three measurements were performed and the second measurement forced through (0, 0).

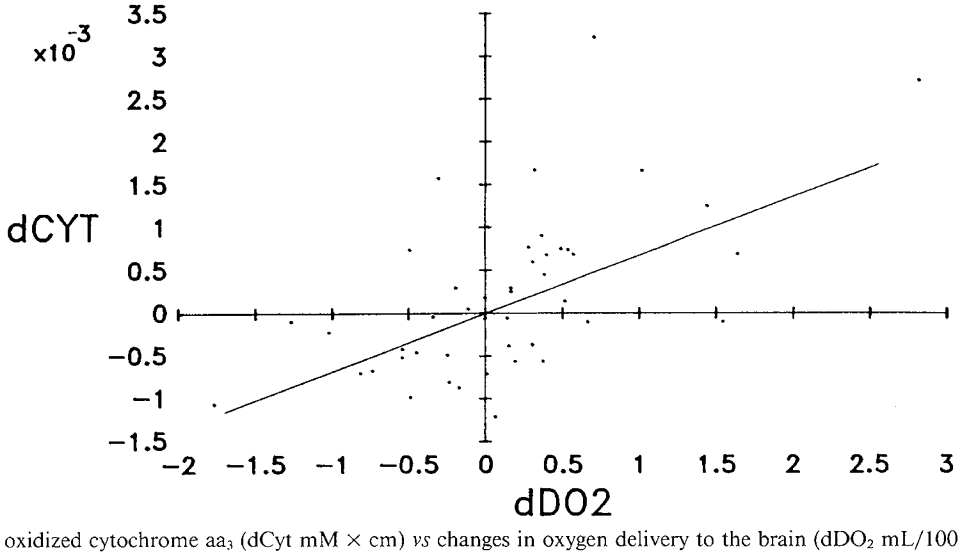

Fig. 3. Changes in oxidized cytochrome aa_3 ($dCyt$ mM × cm) *vs* changes in oxygen delivery to the brain (dDO_2 mL/100 g/min) in 24 preterm infants. In each infant, three measurements were performed and the second measurement forced through (0, 0).

maintenance 5 mg/kg/d) and paralyzed with pancuronium (0.1 mg/kg).

Design. The NIRS optodes were fixed on each side of the infant's head in the frontoparietal region closest to the scintillator. Transillumination mode with the optodes placed symmetrically and pointing toward each other at 180° was attempted, but in some infants with large heads, the optodes had to be closer to obtain an acceptable signal to noise ratio; the optodes were therefore angled at 180 to 150°. The interoptode distance ranged from 5 to 7 cm (not included in the calculations).

When the infant had been undisturbed for about 30 min, the CBF was measured while the NIRS signal was displayed and the data stored for later analysis. During the CBF measurement, MABP was recorded from an umbilical catheter and arterial blood drawn for measuring blood gases, HbC, and SaO_2 (ABL and OSM2, Radiometer). After the measurement, ventilator settings (expiratory time) were adjusted to increase or decrease $PaCO_2$ by ± 1.0 kPa, estimated from transcutaneous Po_2 and Pco_2 electrodes (TCM3, Radiometer), and a new steady state awaited before another measurement was taken. Values of $PaCO_2$ from 3 to 5 kPa were attempted as we recommended. If PaO_2 was out of range (8–10 kPa), the inspiratory fraction of oxygen was adjusted appropriately. The procedure was repeated, resulting in three sets of data from each infant, obtained within about 2 h. The infants were not disturbed during the investigation, and because of muscle paralysis, movement artifacts were avoided.

After the study, mean values of changes in OD at each wavelength, HbTOT, HbO_2, and HbR, and oxidized cytochrome aa_3 were calculated for the 15 min period over which CBF_∞ was measured. An estimate of changes in CBV_I was calculated:

$$100/1.05 \times (\text{change in HbTOT})/\text{HbC}/0.69 \text{ (mL/100 g} \times \text{cm)}$$

where 1.05 is the brain sp gr and 0.69 is the cerebral to large vessel hematocrit ratio (14). The relation between CBV and CBV_I is $CBV = CBV_I/\text{path length}$.

Oxygen delivery to the brain was calculated from the sum of physically dissolved and Hb-bound O_2:

$$((PaO_2 \times 0.227 + SaO_2 \times 84.0 \times \text{HbC})/1000) \times CBF_\infty \text{ (mL } O_2\text{/100 g/min)}.$$

Statistics. First, changes in OD for each wavelength, changes in CBV_I, and changes in CBF_∞ were used as dependent variables introducing $PaCO_2$, MABP, and PaO_2 in a stepwise multiple regression analysis. A variable with 24 levels, one for each infant,

was included (15) to analyze only the intraindividual variability. Next, the relation between changes in OD, CBV_I, and CBF_∞ was analyzed. Finally, the association between changes in cytochrome aa_3 and oxygen delivery was tested.

The Statistical Package for the Social Sciences (Chicago, IL) was used. The study was approved by the Ethics Committee for Greater Copenhagen and parental informed consent obtained for each infant.

RESULTS

CBF_∞ averaged 10.1 mL/100 g/min (SD 4.0) for all the measurements. Mean values of $PaCO_2$, MABP, and pH were 4.4 kPa (SD 1.2), 39.4 mm Hg (SD 8.3), and 7.43 (SD 0.09). Mean changes in $PaCO_2$, MABP, and pH between the serial measurements were 1.2 kPa (SD 0.7), 3.2 mm Hg (SD 2.2), and 0.07 (SD 0.04), respectively. SaO_2 ranged between 0.90 and 1.0 (median 0.95).

Changes in OD versus changes in $PaCO_2$ and CBF_∞. Carbon dioxide-induced increase in CBF_∞ was correlated with increases in OD at 904, 845, 805, and 775 (Table 1). When $PaCO_2$ was introduced in a bivariate regression analysis, changes in CBF_∞ reached a closer relationship to changes in OD than did changes in $PaCO_2$ ($p = 0.0067$ and $p = 0.023$, respectively). Probably, this finding was due to heterogeneity of $CBV_I/CBF\text{-}CO_2$ reactivity among the infants (see below).

Changes in CBV_I versus changes in $PaCO_2$, MABP, and PaO_2. Changes in CBV_I were closely related to changes in $PaCO_2$ ($p < 0.0001$), whereas neither changes in MABP nor PaO_2 reached a significant relationship. In this study, 39.0% of the intraindividual variation of CBV_I was accounted for by changes in $PaCO_2$. Thus, CBV_I increased by a mean of 1.70 mL/100 g × cm (95% CI 1.05 to 2.35) per kPa increase in $PaCO_2$. The $CBV_I\text{-}O_2$ reactivity was calculated to −0.16 mL/100 g × cm per kPa (95% CI −0.43 to 0.10) and the CBV_I-MABP reactivity to 0.05 mL/100 g × cm per mm Hg (95% CI −0.27 to 0.37). In infants investigated during the second day of life, the $CBV_I\text{-}CO_2$ reactivity was 42.0% higher than in infants investigated during the first day of life, but this difference was not significant (Table 2).

The $PaCO_2$-induced changes in CBV_I were due to changes in HbO_2, whereas HbR tended to decrease with increasing $PaCO_2$ (Fig. 1).

Changes in CBF_∞ versus changes in $PaCO_2$, MABP, and PaO_2. The relationship between changes in the three variables and CBF_∞ was similar to that of CBV_I; here, 52.6% of the intraindividual variation of CBV_∞ was explained by changes in $PaCO_2$ ($p < 0.0001$). In addition, a significant difference in $CBF_\infty\text{-}CO_2$ reactivity was found between infants of different ages. Thus, the mean $PaCO_2$ reactivity was 11.9% per kPa during the first day of life and 27.3% per kPa during the second day (Table 2). Changes in PaO_2 and MABP were not significantly related to changes in CBF_∞ ($p = 0.45$ and $p < 0.93$, respectively).

Changes in CBV_I versus changes in CBV_∞. A linear relation was found between changes in CBF_∞ and changes in CBV_I ($r = 0.70$; $p < 0.0001$; Fig. 2). Thus, CBV_I changed by a mean of 0.63 mL/100 g × cm per mL/100 g/min change in CBF_∞ (95% CI 0.40 to 0.87).

Changes in oxidized cytochrome aa_3 versus oxygen delivery. The oxygenation level of cytochrome aa_3 increased linearly with increases in oxygen delivery ($r = 0.72$; $p < 0.0001$) as presented in Fig. 3. The regression coefficient was calculated:

0.0038 mM

× cm per mL/100 g/min (95% CI 0.0020 to 0.0056).

This relationship, however, disappeared when HbO_2 was introduced as a second variable in the statistical analysis, indicating that the estimates of oxidized cytochrome aa_3 and HbO_2 were strongly correlated to each other.

DISCUSSION

In our study, the OD at all four wavelengths increased significantly when CBF_∞ rose at higher $PaCO_2$ levels. This finding is consistent with increasing amounts of absorbants in the brain. The magnitude of each regression coefficient, the lowest observed for 775 nm, indicates that arteriolar dilation occurred, resulting in a higher mean Hb saturation.

Conversion of the recordings to an index of CBV gave a linear relation between changes in CBV_I and CBF_∞ within the observed range of $PaCO_2$ (2.1 to 7.8 kPa), but the changes in CBV_I did not ascertain an age-dependent difference in the $PaCO_2$ reactivity. An attenuated CO_2 reactivity in mechanically ventilated preterm infants during the first day of life has recently been observed (16, 17).

It should be noted that the $CBV_I\text{-}CBV_\infty$ relationship reported in this study may only be valid for $PaCO_2$-induced changes. CBF is determined by MABP, intracranial pressure, blood viscosity, and the diameter of arteries and arterioles. However, CBV is mainly determined by the diameter of venules and arterioles, the latter thus being a common denominator for both CBF and CBV. Changes in the cerebral perfusion pressure may give a different relationship, as may conditions involving changes in the central venous pressure and cerebral venous drainage.

Although changes in CBV_I were closely related to changes in CBF_∞, the data have certain limitations. Quantification of the NIRS recordings to absolute concentrations and CBF presupposes that the light path length is known. However, determination of the path length is not straightforward because of multiple scatterings of light inside the head (18). The scattering effect depends on several factors, *e.g.* cell concentration, myelination, and bone mineralization, implying that the path length is a complex function of the geometrical distance between the optodes (according to the Lambert-Beer law), the amount of scattering elements (gestational age), and the concentration of chromophores. Furthermore, the path length is different for the various wavelengths used (775–904 nm), with a longer path length at shorter wavelengths; this should be taken into account when quantification is attempted. Hopefully, these problems will be clarified in the future. In our study, we attempted to keep the interoptode distance within a narrow range, but our knowledge of the light path length may have optimized the relation between changes in CBV_I and CBF_∞.

The oxygenation level of cytochrome aa_3 correlated with the oxygen delivered to the brain. Inasmuch as changes in oxidized cytochrome aa_3, HbO_2 and oxygen delivery were expected to be highly correlated in the present experimental design, the statistical analysis cannot be conclusive with regard to presence of cross-talk between oxidized cytochrome and oxygenated HbO_2 respectively. Three important considerations should be made. First, if HbO_2 and oxidized cytochrome aa_3 change in parallel, it means that cytochrome aa_3 is partly reduced at normal PaO_2 tensions as previously suggested (19, 20). These studies, however, used the same technique, with the same probability that apparent cytochrome aa_3 redox changes are artifactual. Second, the present algorithm for calculating changes in cytochrome aa_3 is derived from studies of rat brain exchange transfused with fluorocarbon and may therefore be affected by "noise" due to pH transients (which may affect the absorption spectra), fluctuation in scattering (vasodilation during hypoxia), or residual Hb after fluorocarbon exchange. Further *in vitro* and animal studies elaborating these problems are needed. Finally, and perhaps most importantly, the amount of cytochrome aa_3 may be very small in the preterm brain, as the low cerebral activity in preterm neonates implies a low energy requirement for electrical transmission (21). Consequently, fluctuations in redox level of cytochrome aa_3 may be easily masked.

In conclusion, $PaCO_2$-induced changes in CBF_∞ resulted in parallel changes in CBV_I, presumably due to arteriolar dilation of the cerebral vessels. Similarly, increase in oxygen delivery to

the brain was accompanied by increase in the signal of oxidized cytochrome aa_3, but there are reasons to believe this to be artifactual.

Acknowledgments. The Gerda and Åge Haench Foundation and the Dagmar Marschal Foundation gave financial support. The statistical method was provided by the Statistical Research Unit, University of Copenhagen, Copenhagen, Denmark.

REFERENCES

1. Jöbsis FF 1977 Noninvasive infrared monitoring of cerebral and myocardial oxygen sufficiency and circulatory parameters. Science 198:1264–1267
2. Brazy JE, Darrel VL, Mitnick MH, Jöbsis FF 1985 Noninvasive monitoring of cerebral oxygenation in preterm infants: preliminary observations. Pediatrics 75:217–225
3. Wyatt JS, Cope M, Delpy DT, Wray S, Reynolds EOR 1986 Quantification of cerebral oxygenation and haemodynamics in sick new born infants by near infrared spectrophotometry. Lancet 8515:1063–1066
4. Risberg J, Ancri D, Ingvar DH 1969 Correlation between cerebral blood volume and cerebral blood flow in the cat. Exp Brain Res 8:321–326
5. Smith AL, Neufeld GR, Ominsky AJ, Wollman H 1971 Effect of arterial CO_2 tension on cerebral blood volume, mean transit time, and vascular volume. J Appl Physiol 31:701–707
6. Phelps ME, Grubb RL, Ter-Pogossian MM 1973 Correlation between $PaCO_2$ and regional cerebral blood volume by x-ray fluorescence. J Appl Physiol 35:274–280
7. Takashima S, Ando Y 1988 Reflectance spectrophotometry, cerebral blood flow and congestion in young rabbit brain. Brain Dev 10:20–23
8. Greenberg JH, Alavi A, Reivich M, Kuhl D, Uzzell B 1978 Local cerebral blood volume response to carbon dioxide in man. Circ Res 43:324–331
9. Lassen NA 1974 Control of cerebral circulation in health and disease. Circ Res 34:749–760
10. Wray S, Cope M, Delpy DT, Wyatt JS, Reynolds EOR 1988 Characterization of the near infrared absorption spectra of cytochrome aa_3 and haemoglobin for the non-invasive monitoring of cerebral oxygenation. Biochim Biophys Acta 933:184–192
11. Greisen G, Pryds O 1988 Intravenous ^{133}Xe clearance in preterm neonates with respiratory distress. Internal validation of CBF_∞ as a measure of global cerebral blood flow. Scand J Clin Lab Invest 48:673–678
12. Obrist W, Thompson HK, Wang HS, Wilkinson WE 1975 Regional cerebral blood flow estimated by $^{133}Xenon$ inhalation. Stroke 6:245–256
13. Greisen G 1986 Cerebral blood flow in preterm infants during the first week of life. Acta Paediatr Scand 75:43–51
14. Lammertsma AA, Brooks DJ, Beany RP, Turton DR, Kenset MJ, Heather JD, Marshall J, Jones T 1984 *In vivo* measurements of regional cerebral haematocrit using positron emission tomography. J Cereb Blood Flow Metab 4:317–322
15. Smith EO 1987 Analysis of repeated measures designs (editorial). J Pediatrics 111:723–725
16. Levene M, Shortland D, Gibson N, Evans DH 1988 Carbon dioxide reactivity of the cerebral circulation in extremely premature infants: effects of postnatal age and indomethacin. Pediatr Res 24:175–179
17. Pryds O, Greisen G, Lou H, Friis-Hansen B 1989 Heterogeneity of cerebral blood flow in mechanically ventilated, preterm infants. J Pediatr 115:638–645
18. Delpy DT, Cope M, van der Zee P, Wray S, Wyatt JT 1988 Estimation of optical pathlength through tissue from direct time of flight measurement. Phys Med Biol 33:1433–1442
19. Piantadosi CA, Hemstreet TM, Jöbsis-Vandervliet FF 1986 Near-infrared spectrophotometric monitoring of oxygen distribution to intact brain and skeletal muscle tissues. Crit Care Med 14:698–706
20. Thorniley MS, Wickramasinghe YABD, Rolfe P 1988 Near infra-red spectroscopy: a new technique for the non-invasive monitoring of tissue and blood oxygenation *in vivo*. Biochem Soc Trans 16:978–979
21. Astrup J 1982 Energy-requiring cell functions in the ischaemic brain. J Neurosurg 56:482–497